

High-Frequency Energy Distribution of a Plasma Coated Paraboloid Reflector

Muhammad H. Shahzad¹, Abdul Ghaffar^{1, *}, Muhammad Y. Naz¹, and Haq N. Bhatti²

Abstract—This paper analyzes the high-frequency energy distribution of a paraboloid reflector in the presence of a uniform plasma layer. The curved surface of the paraboloid reflector is thought to be coated with a uniform plasma layer. The geometrical optics technique shows a singularity at the focal point of the paraboloid reflector. The singularity is removed with the help of Maslov’s method, which also let us derive the integral equations that give the high-frequency energy distribution at the focal point. The analytical integral is solved numerically using a computational technique, and the effects of plasma frequency, collisional frequency, operating frequency, and multiple reflections on energy distribution at the focal point are observed. Under the special conditions our analytical and numerical results are obtained which align with the published literature.

1. INTRODUCTION

The communication system’s expansion is progressing quickly, and its performance can be enhanced as a reconfigurable system as plasma antenna [1]. The plasma based reflecting systems or antenna are the future of communication technology, and its characteristics depend upon propagation of electromagnetic waves through plasma environment [2, 3]. The reconfigurable system has the mechanical and electrical control capabilities that enhance the pattern, shape, and performance, and reduce the cost [4]. Many researchers have studied the interaction of electromagnetic waves with tunable plasma material; this area of research has received valuable attention and is a “hot topic” in plasma technology [5–10]. The enhanced performance of absorption, transmission, and the optical reflection of stealth applications, radio astronomy, and radio communication may be obtained using plasma as a cover layer on a communication system [11, 12]. Moreover, when a space vehicle reenters the atmosphere at hypersonic speed, it is wrapped by a plasma sheath due to highly ionized gases [13–15]. The presence of so many free electrons in the plasma sheath causes significant attenuation in radio frequency through absorption and reflection [16]. First, this plasma sheath creates a communication black-out phenomenon that affects the communication system’s performance. The communication black-out phenomenon significantly reduces the signal intensity.

The antenna affected in beamforming and pointing due to the presence of the plasma sheath is reflective and glossy; this effect alters and distorts the field distribution due to the attenuation and phase delay in the propagation of EM waves in different directions after passing through the plasma sheath [14]. Second, mutual coupling increases, and the input impedance is altered due to the plasma sheath’s reflective property [17]. Therefore, the radiation pattern will be distorted, and beam pointing errors will increase. Therefore, it is necessary to study the effect of the plasma layer on the paraboloid reflector field distribution in the focal region. There are many theoretical techniques to study field intensity distribution in the caustic region of any dielectric coated reflector, and one of them

Received 24 February 2020, Accepted 22 April 2020, Scheduled 29 April 2020

* Corresponding author: Abdul Ghaffar (aghaffar16@uaf.edu.pk).

¹ Department of Physics, University of Agriculture, Faisalabad, Pakistan. ² Department of Chemistry, University of Agriculture, Faisalabad, Pakistan.

is geometrical optics (GO). The GO is based on ray theory and unable to show results at focal point due to the singularity's physical appearance. Therefore, an alternative technique known as "Maslov's method" removes the singularity at the focal point of the GO field [18,19]. This technique provides an integral solution that combines the generality of a Fourier transform with the simplicity of the ray. Many authors have used Maslov's method to carry out this type of research [20–24].

The reflection and transmission of electromagnetic waves may be affected by the surface charged particles on the surface, which was pointed out by many researchers [25–30]. These effects may be significant for charged particles as compared to uncharged particles. The net surface charges toward the reflection and transmission of electromagnetic waves from the surface occur due to the static electric dipole induction. The strength of net surface charges vanishes when overall the particles charge uniformly due to symmetry [31]. The effects of net surface on all the field reflected or transmitted become zero when the particles on the surface of reflecting or transmitting system are completely charged uniformly. The presence of plasma layer in the form of charged particles on the surface of reflector may alter the field distribution due to the attenuation and phase delay in the propagation of EM waves in different directions after passing through the plasma.

In this study, we consider a metallic paraboloid reflector coated with a uniform un-magnetized plasma material under normal incidence and ignore the above stated net surface charges. This study provides the exact distribution of the high-frequency energy distribution in the paraboloid reflector coated with a plasma material around focal point or caustic point, with the help of Maslov's method. The plasma thickness, plasma frequency, and operating frequency's effects on the energy distributions of the plasma-layered paraboloid near the focal regions are also deliberated. The described effects on field energy distribution are studied using numerical computations. The analytical and numerical results are confirmed from the literature under special conditions. The $(j\omega t)$ time dependency is taken and omitted in the following.

2. FORMULATIONS

A perfect metallic paraboloid reflector coated with a uniform isotropic plasma cover is considered. The geometry of the plasma-coated paraboloid is displayed in Figure 1, and the surface equation of the paraboloid without a coat is:

$$\zeta_0 = \frac{4f^2 - \rho_0^2}{4f} \quad (1)$$

where $\rho_0 = \sqrt{\xi_0^2 + \eta_0^2}$ with ξ_0 , η_0 , and ζ_0 as the surface coordinates of the metallic paraboloid reflector, and f as the focal length. The surface equation of the plasma-coated metallic paraboloid reflector is written as

$$\zeta = \frac{4f(f-d) - \rho^2}{4f} \quad (2)$$

where d is the width of the plasma coat, $\rho = \sqrt{\xi^2 + \eta^2}$ with ξ , η , and ζ as the surface coordinates of the plasma-coated paraboloid.

A perpendicularly polarized plane electromagnetic wave in the x direction incident normally to the plasma-coated paraboloid is

$$E_i(r) = \hat{x}E_i(r)e^{-ik_i z} \quad (3)$$

The plane EM wave is reflected and transmitted at free-space-plasma curved interfaces. The transmitted electromagnetic wave propagates toward the metallic curved paraboloid surface and reflects back toward the plasma-free-space interface. Through this, multiple reflections can occur from the metallic paraboloid surface, and multiple refractions can occur from the plasma to the free space, and rays approach the focal point. The reflected wave vectors R and transmitted wave vectors T can be obtained using Snell's laws

$$R = -\sin 2\alpha \cos \beta i_x - \sin 2\alpha \sin \beta i_y - \cos 2\alpha i_z \quad (4)$$

$$T = \left(\sqrt{\cos^2 \alpha - \frac{\omega_p^2}{\omega^2}} - \cos \alpha \right) (\cos \beta \sin \alpha i_x + \sin \beta \sin \alpha i_y + \cos \alpha i_z) + i_z \quad (5)$$

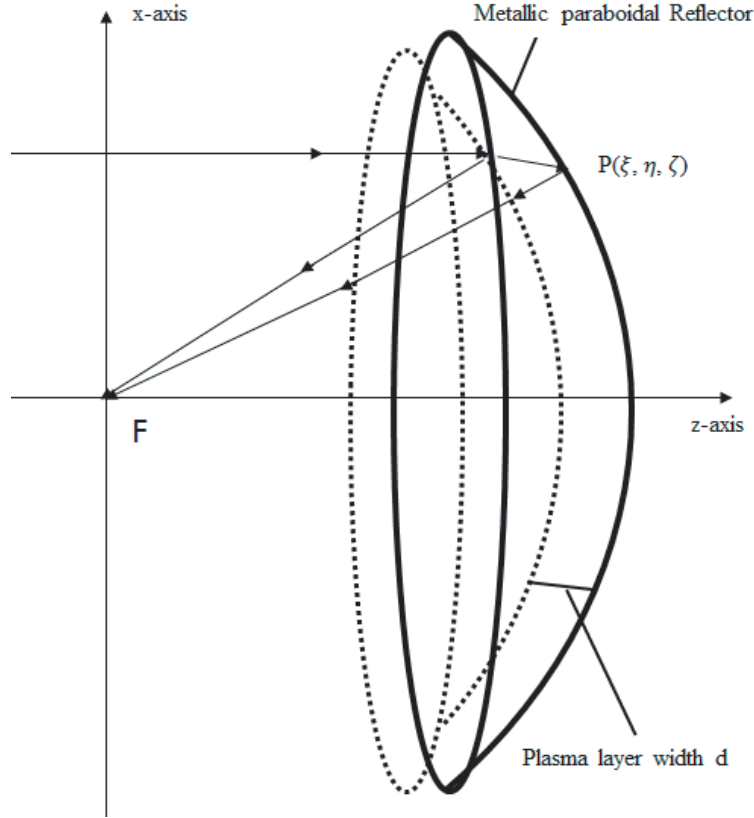


Figure 1. Plasma-coated paraboloid antenna.

where α and β are the angular coordinates of paraboloid. Similarly, the T wave vector hits the curved metallic paraboloid and is reflected back as a R_1 wave vector inside the plasma layer toward the plasma-free-space interface. In addition, it refracts with the T_1 wave vector toward the focal point F . The expressions for R_1 and T_1 can be obtained by Snell's laws

$$R_1 = -X_1 \cos \beta \sin \alpha i_x + X_1 \sin \beta \sin \alpha i_y + \left(\sin^2 \alpha - \cos \alpha \sqrt{\cos^2 \alpha - \frac{j\omega_p^2}{(v+j\omega)\omega}} \right) i_z \quad (6)$$

$$T_1 = (X_2 - \cos \alpha) (\cos \beta \sin \alpha i_x + \sin \beta \sin \alpha i_y) + (\sin^2 \alpha + \cos \alpha X_2) i_z \quad (7)$$

where $X_1 = \sqrt{\cos^2 \alpha - \frac{j\omega_p^2}{(v+j\omega)\omega}} + \cos \alpha$ and $X_2 = \sqrt{\cos^2 \alpha - \frac{2j\omega_p^2}{(v+j\omega)\omega}} - 2\sqrt{\cos^2 \alpha - \frac{j\omega_p^2}{(v+j\omega)\omega}}$; v is the collisional frequency, ω_p the plasma frequency, and ω the operating frequency of the EM plane wave.

The solutions of Hamilton's equations are obtained at the focal point F for the reflected and transmitted rays

$$x = \xi + R_x \tau_1, \quad y = \eta + R_y \tau_1, \quad z = \zeta + R_z \tau_1 \quad (8)$$

$$x = \xi + T_{1x} \tau_2, \quad y = \eta + T_{1y} \tau_2, \quad z = \zeta + T_{1z} \tau_2 \quad (9)$$

where τ_1 and τ_2 are respectively the path length of the reflected wave and the transmitted wave from the paraboloid plasma layer to the caustic point. The Jacobian of the refracted ray from the plasma layered paraboloid is

$$D(\tau_2) = \frac{\partial(x, y, z)}{\partial(\xi, \eta, \tau_2)} = \begin{vmatrix} 1 + \frac{\partial T_{1x}}{\partial \xi} \tau_2 & \frac{\partial T_{1y}}{\partial \xi} \tau_2 & \frac{\partial \zeta}{\partial \xi} + \frac{\partial T_{1z}}{\partial \xi} \tau_2 \\ \frac{\partial T_{1x}}{\partial \eta} \tau_2 & 1 + \frac{\partial T_{1y}}{\partial \eta} \tau_2 & \frac{\partial \zeta}{\partial \eta} + \frac{\partial T_{1z}}{\partial \eta} \tau_2 \\ T_{1x} & T_{1y} & T_{1z} \end{vmatrix} \quad (10a)$$

$$J(\tau) = \frac{D(\tau_2)}{D(0)} \quad (10b)$$

The geometric optics field expressions for transmitted rays out of the paraboloid plasma layer are

$$E_r(x, z) = E_i[J(\tau_2)]^{-\frac{1}{2}} \exp[-jk(-\zeta + \tau_2)] \quad (11)$$

As expected, we can observe the above field becoming infinite when $J(\tau_1) = 0$ at the focal points. Maslov's method may be used here to avoid a singularity. The field expression with help from Maslov's method is as follows:

$$E^t(r) = \frac{k}{2\pi} \int_{-\infty}^{\infty} \int_{-\infty}^{\infty} E^{t0} \left[\frac{D\tau_2}{D(0)} \frac{\partial(T_{1x}, T_{1y})}{\partial(x, y)} \right]^{-\frac{1}{2}} \times \exp\{jk[S_0 + \tau_2 - x(T_{1x}, T_{1y}, z)T_{1x} - y(T_{1x}, T_{1y}, z)T_{1y} + T_{1x}x + T_{1y}y]\} dT_{1x}dT_{1y} \quad (12)$$

The phase function $S(T_{1x}, T_{1y})$ of the integral in Eq. (12) is given by

$$\begin{aligned} S(T_{1x}, T_{1y}) &= -\zeta + \frac{z - \zeta}{T_{1z}} - (\xi + T_{1x})T_{1x} - (\eta + T_{1y})T_{1y} + T_{1x}x + T_{1y}y \\ &= \zeta - \xi T_{1x} - \eta T_{1y} - \zeta T_{1z} + T_{1x}x + T_{1y}y + T_{1z}z \end{aligned} \quad (C1)$$

as we have

$$\xi = 2f \cos \beta \tan \alpha, \quad \eta = 2f \sin \beta \tan \alpha, \quad \zeta = f \frac{\cos 2\alpha}{\cos^2 \alpha} \quad (C2)$$

and the polar coordinates

$$x = r \cos \varphi \sin \theta, \quad y = r \sin \varphi \sin \theta, \quad z = r \cos \theta \quad (C3)$$

The ray vector components $(T_{1x}T_{1y}T_{1z})$ are written below

$$\left. \begin{aligned} T_{1x} &= \cos \beta \sin \alpha (-\cos \alpha + X_2) \\ T_{1y} &= \sin \beta \sin \alpha (-\cos \alpha + X_2) \\ T_{1z} &= \sin^2 \alpha + \cos \alpha X_2 \end{aligned} \right\} \quad (C4)$$

Using Eqs. (C2) and (C4) we get

$$\zeta - \xi T_{1x} - \eta T_{1y} - \zeta T_{1z} = f - fX_2 \sec \alpha \quad (C5)$$

$$T_{1x}x + T_{1y}y + T_{1z}z = r (\cos \theta (X_2 \cos \alpha + \sin^2 \alpha) + (X_2 - \cos \alpha) \cos (\beta - \varphi) \sin \alpha \sin \theta) \quad (C6)$$

Putting Eqs. (C5) and (C6) into Eq. (C1), we now have transmission

$$S = f - fX_2 \sec \alpha + r \cos \theta (X_2 \cos \alpha + \sin^2 \alpha) + r (X_2 - \cos \alpha) \cos (\beta - \varphi) \sin \alpha \sin \theta \quad (13)$$

The amplitude of the integrand is

$$\begin{aligned} J(\tau) \frac{\partial(T_{1x}, T_{1y})}{\partial(x, y)} &= \frac{1}{D(0)} \frac{\partial(T_{1x}, T_{1y}, z)}{\partial(\xi, \eta, \tau_2)} \\ &= \frac{(X_2 - \cos \alpha) \cos^4 \alpha (X_2 \cos \alpha + \sin^2 \alpha) (-\cos 2\alpha + \cos \alpha (X_2 + \sqrt{2}X_3 \sin^2 \alpha))}{4f^2 X_2} \end{aligned} \quad (14)$$

Changing (ξ, η) to angular coordinates (α, β) by

$$\frac{\partial(\alpha, \beta)}{\partial(\xi, \eta)} = \frac{\cos^3 \alpha}{4f^2 \sin \alpha} \quad (15)$$

The relationship between Cartesian (T_{1x}, T_{1y}) coordinates and surface coordinates (ξ, η) is

$$\frac{\partial(T_{1x}, T_{1y})}{\partial(\xi, \eta)} = \frac{(X_2 - \cos \alpha) \cos^3 \alpha (-\cos 2\alpha + \cos \alpha (X_2 + \sqrt{2}X_3 \sin^2 \alpha))}{4f^2} \quad (16)$$

Using Equations (13) to (16) and the final field expression in Equation (12), the final field expressions are obtained as

$$E^r(r) = \frac{2jkf}{\pi} \int_0^T \int_0^{2\pi} E_{t0} \sqrt{\frac{(X_2 - \cos \alpha)(-\cos 2\alpha + \cos \alpha(X_2 + \sqrt{2}X_3 \sin^2 \alpha))}{\cos \alpha(X_2 \cos \alpha + \sin^2 \alpha)}} \tan \alpha \times \exp\{-jk(f - fX_2 \sec \alpha + r \cos \theta(X_2 \cos \alpha + \sin^2 \alpha) + r(X_2 - \cos \alpha) \cos(\beta - \varphi) \sin \alpha \sin \theta)\} d\alpha d\beta \quad (17)$$

The integral is solved analytically over variable β , and we get:

$$E_x(r) = jkf E_{t0} e^{-jkf} (P_1(r, \theta) + P_2(r, \theta) \cos 2\varphi) \quad (18a)$$

$$E_y(r) = jkf E_{t0} e^{-jkf} P_2(r, \theta) \sin 2\varphi \quad (18b)$$

$$E_z(r) = jkf E_{t0} e^{-jkf} P_3(r, \theta) \cos \varphi \quad (18c)$$

$$P_1(r, \theta) = \frac{kf}{\pi} \int_0^T \sqrt{\frac{(X_2 - \cos \alpha)(-\cos 2\alpha + \cos \alpha(X_2 + \sqrt{2}X_3 \sin^2 \alpha))}{\cos \alpha(X_2 \cos \alpha + \sin^2 \alpha)}} \sin 2\alpha J_0(r(X_2 - \cos \alpha) \sin \alpha \sin \theta) \exp\{-jk(-fX_2 \sec \alpha + r \cos \theta(X_2 \cos \alpha + \sin^2 \alpha))\} d\alpha$$

$$P_2(r, \theta) = \frac{2kf}{\pi} \int_0^T \sqrt{\frac{(X_2 - \cos \alpha)(-\cos 2\alpha + \cos \alpha(X_2 + \sqrt{2}X_3 \sin^2 \alpha))}{\cos \alpha(X_2 \cos \alpha + \sin^2 \alpha)}} \sin^2 \alpha \tan \alpha J_2(r(X_2 - \cos \alpha) \sin \alpha \sin \theta) \exp\{-jk(-fX_2 \sec \alpha + r \cos \theta(X_2 \cos \alpha + \sin^2 \alpha))\} d\alpha$$

$$P_3(r, \theta) = \frac{2kf}{\pi} \int_0^T \sqrt{\frac{(X_2 - \cos \alpha)(-\cos 2\alpha + \cos \alpha(X_2 + \sqrt{2}X_3 \sin^2 \alpha))}{\cos \alpha(X_2 \cos \alpha + \sin^2 \alpha)}} \sin 2\alpha \tan \alpha J_1(r(X_2 - \cos \alpha) \sin \alpha \sin \theta) \exp\{-jk(-fX_2 \sec \alpha + r \cos \theta(X_2 \cos \alpha + \sin^2 \alpha))\} d\alpha$$

where T is the angle with the aperture. The transmission coefficients are obtained using the boundary conditions at the curved free-space-curved paraboloid plasma interface at $z = \zeta$. There are several bounces inside the plasma-coated layer at plasma-metal interface and plasma-free-space interface. Similarly, there are several transmissions at the plasma-free-space boundary. The first reflection coefficient Γ_{12} and first transmission coefficient T_{21} at the curved free-space-curved plasma interface can be obtained respectively as

$$\Gamma_{12} = \frac{1 - n}{1 + n} e^{-j2k\zeta} \quad (19)$$

$$T_{21} = \frac{2n}{1 + n} e^{-j(-k\zeta n + k\zeta)} \quad (20)$$

The transmitted wave propagates inside the plasma coat and incident at the metallic paraboloid reflector and bounces back toward the free-space-plasma boundary. The reflected coefficient Γ_{23} at the plasma-metal boundary is

$$\Gamma_{23} = -T_{21} e^{j2k\zeta n} \quad (21)$$

Since there are multiple reflections within the plasma layer, the total transmission coefficient in the geometric series [32, 33] is

$$E_{t0} = \Gamma_{12} + \frac{(1 - T_{21}\Gamma_{23} \exp(-2jk\zeta_0 n))^m}{1 - \Gamma_{21}\Gamma_{23} \exp(-2jk\zeta_0 n)} \times T_{12} T_{21} \Gamma_{23} \exp(-2jk\zeta) \quad (22)$$

where $m = 1, 2, 3 \dots$ for multiple bounces of rays inside the plasma layer.

Interestingly, we can observe that the above integrals expression approaches the analytical and numerical results represented by Equations (41a), (41b), and (41c) of [20] if the plasma frequency $\omega_p = 0$.

3. RESULTS AND DISCUSSION

The above analytical study was developed to calculate the high-frequency energy distribution of the paraboloid reflector in the presence of a uniform plasma layer under normal incidence. The energy distribution of a paraboloid reflector along the focal region is obtained by numerically solving $|E(r)|^2 = |E_x^2(r) + E_y^2(r) + E_z^2(r)|$ with Mathematica software. The energy distribution of a paraboloid reflector is obtained with the help of Maslov's method, which is a successful method that combines geometrical optics and the Fourier transform method [16–21]. Our work's accuracy can be verified by considering the plasma frequency $\omega_p = 0$. Each of our obtained expressions will transform precisely as the expressions obtained in [20]. Figure 2 shows the computational results of our developed analytical expression at plasma frequency $\omega_p = 0$ and the field expression obtained at [20]; they are in agreement. After verifying our work's validity, analysis is carried out in the following paragraphs.

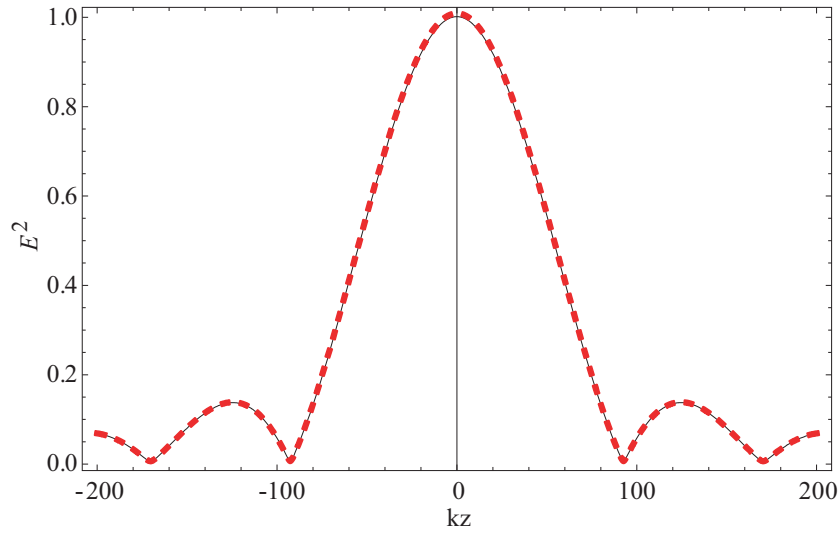


Figure 2. Comparison of the electric field distribution in the focal region w.r. to z -axis of our work (solid line) at $\omega_p = 0$ and $\omega_p = 0$ [21] (dashed line).

Figure 3 illustrates the energy distribution of the paraboloid reflector in the presence of a uniform plasma layer under normal incidence around the focal point with respect to the z -axis for different values of plasma electron densities $n_e = 30 \times 10^{12}$, 25×10^{12} , 20×10^{12} , and 15×10^{12} at the operating frequency $\omega = 1 \times 10^6$ Hz, collisional frequency $\nu = 5 \times 10^{10}$ Hz, $kf = 5$, $ka = 10$, and plasma thickness $kd = 0.01$. In this figure, the energy distribution of the paraboloid reflector is evidently higher at higher values of the plasma electron density at the focal point along the z -axis due to good matching between the electromagnetic wave and the plasma; this matching occurs by increasing the electron density in the direction of propagation. At the decreasing value $n_e = 1 \times 10^{12}$, the plasma layer behaves as a PEC reflector, and the increasing value behaves as a non-reflecting medium.

Figure 4 illustrates the energy distribution of the paraboloid reflector in the presence of a uniform plasma layer under normal incidence around the focal point with respect to the operating frequency ω for different plasma electron densities $\omega_p = 12 \times 10^9$ Hz, 11×10^9 Hz, 10×10^9 Hz, and 9×10^9 Hz at $z = f$, collisional frequency $\nu = 5 \times 10^{10}$ Hz, $kf = 20$, $ka = 10$, and plasma thickness $kd = 0.01$. In this figure, the energy distribution of the paraboloid reflector is evidently lower at higher plasma frequency values. We also observe that the energy distribution of the paraboloid reflector is concentrated within the operating frequency range bandgap of -0.05 GHz. Note that at a lower plasma frequency, the maximum energy is transmitted due to a very small reflection. Therefore, nearly all of the electric field intensity is absorbed or transmitted according to the operating frequency of an electromagnetic wave with ignorable reflection.

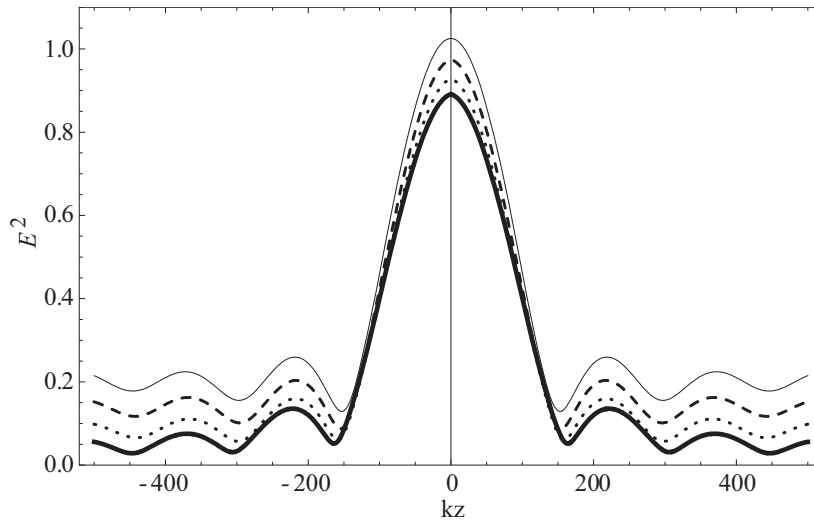


Figure 3. Electric field distribution at $\omega = 1 \times 10^6$ Hz in the focal region along the z -axis for different values of plasma electron densities $n_e = 30 \times 10^{12} \text{ m}^{-3}$ (thin solid), $25 \times 10^{12} \text{ m}^{-3}$ (dashed), $20 \times 10^{12} \text{ m}^{-3}$ (dotted), $415 \times 10^{12} \text{ m}^{-3}$ (thick solid).

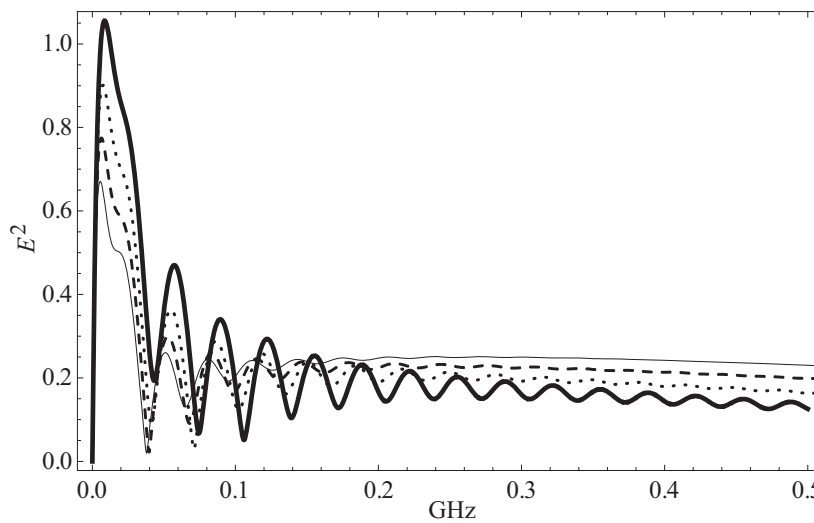


Figure 4. Electric field distribution in the focal region w.r.to operating frequency for different plasma frequency values $\omega_p = 12 \times 10^{12}$ Hz (thin solid), 11×10^{12} Hz (dashed), 11×10^{12} Hz (dotted), 10×10^{12} Hz (thick solid).

Figure 5 illustrates the energy distribution of the paraboloid reflector in the presence of a uniform plasma layer under normal incidence with respect to the operating frequency ω for different values of the plasma collisional frequency $\nu = 5 \times 10^{11}$ Hz (thin solid), 4×10^{11} Hz (dashed), 3×10^{11} Hz (dotted), 2×10^{11} Hz (thick solid) at $z = f$, plasma frequency $\omega_p = 9 \times 10^9$ Hz, $kf = 10$, $ka = 20$, and plasma thickness $kd = 0.01$. This figure shows that the energy distribution of the paraboloid reflector is higher at higher values for the plasma frequency. Note that the plasma layer is more likely to be a good reflector as the collisional frequency decreases. We conclude that the reflected electric field intensity increases as the collisional frequency decreases. Note that the bandwidth of the reflected energy distribution and transmitted energy distribution characteristics change considerably for a selected value of the maximum electron density and collision frequency.

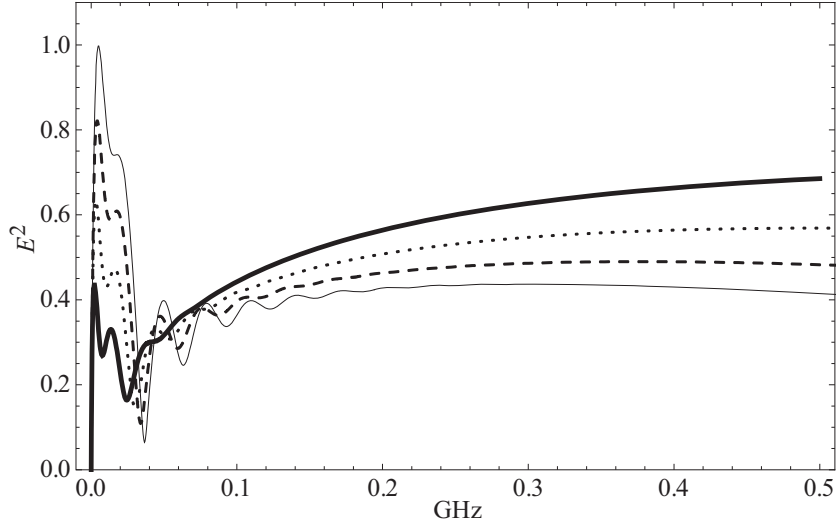


Figure 5. Electric field distribution in the focal region w.r.to operating frequency for different plasma frequency values $\nu = 5 \times 10^{11}$ Hz (thin solid), 4×10^{11} Hz (dashed), 3×10^{11} Hz (dotted), 2×10^{11} Hz (thick solid).

4. CONCLUSION

This study presents theoretical analyses of the electromagnetic fields in the focal region of a metallic paraboloid reflector in the presence of a uniform plasma layer under a normal incident angle. The field intensity distribution components near the focal point are derived using Maslov's method. The reflected and transmitted fields focused at the focal point of the plasma coated paraboloid reflector are in good agreement with the available literature under special conditions. The effects of the plasma, collisional and wave frequency on the transmitted energy distribution are examined. The focused field intensities decrease as the plasma frequency decreases. In the results presented, the effects of multiple reflections inside the layer are considered, and we observe that multiple reflections inside the layer are ignorable due to high loss by the plasma itself. We conclude that tuning the plasma parameters such as the electron number density and collisional frequency means that the proposed plasma layer may be used as a broadband transmitter in stealth applications.

The plasma coated paraboloid has potential application as a possibility for fast switching of working frequency in mobile communication. In defence technology plasma layer ability of de-energizing and energizing in microsecond may behave as a dielectric tube having small scattering radar cross section which causes difficulty to detect from hostile radar. It is very helpful in electronic warfare that when plasma frequency is lower it becomes transparent for higher frequency band, and dangerous signals may pass without interfering the reception and transmission. The plasma coated reflector is also useful in satellite communication due to its steering and fast beam focusing property.

ACKNOWLEDGMENT

Authors would like to thank Higher Education Commission (HEC) under NRPDU for under Project No. 8576.

REFERENCES

1. Alexeff, I., T. Anderson, E. Farshi, N. Karnam, and N. R. Pulasani, "Recent results for plasma antennas," *Physics of Plasmas*, Vol. 15, 057104, 2008.
2. Kuz'min, G., I. Minaev, K. Rukhadze, V. Tarakanov, and O. Tikhonovich, "Reflector plasma array antennas," *Journal of Communications Technology and Electronics*, Vol. 57, 536–542, 2012.

3. Alexeff, I., T. Anderson, S. Parameswaran, E. P. Pradeep, J. Hulloli, and P. Hulloli, "Experimental and theoretical results with plasma antennas," *IEEE Transactions on Plasma Science*, Vol. 34, 166–172, 2006.
4. Jusoh, M. T., K. A. Ahmad, M. F. M. Din, and F. R. Hashim, "Reconfigurable antenna using plasma reflector," *AIP Conference Proceedings*, 020029, 2018.
5. Ginzburg, V. L., "The propagation of electromagnetic waves in plasmas," *International Series of Monographs in Electromagnetic Waves*, 2nd Rev. and Enl. Edition, Pergamon, Oxford, 1970.
6. Woods, L., *The Propagation of Electromagnetic Waves in Plasmas*, JSTOR, 1972.
7. Heald, M. A. and C. Wharton, *Plasma Diagnostics with Microwaves*, RE Krieger Pub. Co., 1978.
8. Gradov, O. and L. Stenflo, "On the parametric transparency of a magnetized plasma slab," *Physics Letters A*, Vol. 83, 257–258, 1981.
9. Vidmar, R., "On the use of atmospheric plasmas as electromagnetic reflectors," *IEEE Transactions on Plasma Science*, Vol. 21, 876–880, 1992.
10. Smilyanskii, V., "Propagation of an electromagnetic wave across a magnetic field in a parabolic plasma layer," *Journal of Applied Mechanics and Technical Physics*, Vol. 12, 366–371, 1971.
11. Bai, B., X. Li, Y. Liu, J. Xu, L. Shi, and K. Xie, "Effects of reentry plasma sheath on the polarization properties of obliquely incident EM waves," *IEEE Transactions on Plasma Science*, Vol. 42, 3365–3372, 2014.
12. Jazi, B., B. Davoudi-Rahaghi, M. R. Khajehmirzaei, and A. R. Niknam, "Energy distribution along the focal axis of a metallic cylindrical parabolic reflector covered with a plasma layer," *IEEE Transactions on Plasma Science*, Vol. 42, 286–292, 2014.
13. Bai, B., Y. Liu, X. Lin, and X. Li, "Effects of a reentry plasma sheath on the beam pointing properties of an array antenna," *AIP Advances*, Vol. 8, 035023, 2018.
14. Mei, J. and Y.-J. Xie, "Effects of a hypersonic plasma sheath on the performances of dipole antenna and horn antenna," *IEEE Transactions on Plasma Science*, Vol. 45, 364–371, 2017.
15. Niknam, A., M. Khajehmirzaei, B. Davoudi-Rahaghi, Z. Rahmani, B. Jazi, and A. Abdoli-Arani, "Electromagnetic modeling of the energy distribution of a metallic cylindrical parabolic reflector covered with a magnetized plasma layer," *Physics of Plasmas*, Vol. 21, 073107, 2014.
16. Wang, Z.-B., B.-W. Li, Q.-Y. Nie, X.-G. Wang, and F.-R. Kong, "Study on the electromagnetic waves propagation characteristics in partially ionized plasma slabs," *AIP Advances*, Vol. 6, 055312, 2016.
17. Bai, B., X. Li, Y. Liu, and J. Xu, "Effects of reentry plasma sheath on mutual-coupling property of array antenna," *International Journal of Antennas and Propagation*, Vol. 2015, 2015.
18. Ziolkowski, R. W. and G. A. Deschamps, "Asymptotic evaluation of high-frequency fields near a caustic: An introduction to Maslov's method," *Radio Science*, Vol. 19, 1001–1025, 1984.
19. Thomson, C. and C. Chapman, "An introduction to Maslov's asymptotic method," *Geophysical Journal International*, Vol. 83, 143–168, 1985.
20. Hongo, K., Y. Ji, and E. Nakajima, "High-frequency expression for the field in the caustic region of a reflector using Maslov's method," *Radio Science*, Vol. 21, 911–919, 1986.
21. Hongo, K. and Y. Ji, "High-frequency expression for the field in the caustic region of a cylindrical reflector using Maslov's method," *Radio Science*, Vol. 22, 357–366, 1987.
22. Ghaffar, A. and M. A. Alkanhal, "Fields in the focal region of an elliptical reflector coated with an unmagnetized plasma layer," *Waves in Random and Complex Media*, Vol. 25, 405–416, 2015.
23. Ghaffar, A. and M. A. Alkanhal, "Electromagnetic field intensity distribution along the focal region of a metallic parabolic reflector covered with a plasma layer under oblique incidence," *IEEE Transactions on Plasma Science*, Vol. 43, 3801–3807, 2015.
24. Ghaffar, A. and M. Alkanhal, "Electromagnetic field intensity distribution along focal region of a metallic circular reflector covered with a plasma layer," *Journal of the European Optical Society-Rapid Publications*, Vol. 10, 2015.
25. Bohren, C. F. and A. J. Hunt, "Scattering of electromagnetic waves by a charged sphere," *Canadian Journal of Physics*, Vol. 55, 1930–1935, 1977.

26. Klačka, J. and M. Kocifaj, "Scattering of electromagnetic waves by charged spheres and some physical consequences," *Journal of Quantitative Spectroscopy and Radiative Transfer*, Vol. 106, 170–183, 2007.
27. Klačka, J. and M. Kocifaj, "On the scattering of electromagnetic waves by a charged sphere," *Progress In Electromagnetics Research*, Vol. 109, 17–35, 2010.
28. Kocifaj, M. and J. Klačka, "Scattering of electromagnetic waves by charged spheres: Near-field external intensity distribution," *Optics Letters*, Vol. 37, 265–267, 2012.
29. Klačka, J., M. Kocifaj, F. Kundracik, G. Videen, and I. Kohút, "Generalization of electromagnetic scattering by charged grains through incorporation of interband and intraband effects," *Optics Letters*, Vol. 40, 5070–5073, 2015.
30. Kocifaj, M., J. Klačka, F. Kundracik, and G. Videen, "Charge-induced electromagnetic resonances in nanoparticles," *Annalen der Physik*, Vol. 527, 765–769, 2015.
31. Zhou, J., X. Dou, and L. Xie, "Scattering and attenuation of electromagnetic waves by partly charged particles," *Journal of Quantitative Spectroscopy and Radiative Transfer*, Vol. 206, 55–62, 2018.
32. Gurel, C. S. and E. Oncu, "Characteristics of electromagnetic wave propagation through a magnetised plasma slab with linearly varying electron density," *Progress In Electromagnetics Research B*, Vol. 21, 385–398, 2010.
33. Balanis, C. A., *Advanced Electromagnetic Engineering*, John Wiley & Sons Comp., Hoboken, 1989.